

# Measuring galaxy potentials using shell kinematics

Michael R. Merrifield<sup>1</sup> and Konrad Kuijken<sup>2,3</sup>

<sup>1</sup>*Dept. of Physics and Astronomy, University of Southampton, S017 1BJ*

<sup>2</sup>*Kapteyn Instituut, P.O. Box 800, 9700 AV, Groningen, Netherlands*

<sup>3</sup>*Visiting Scientist, Dept. of Theoretical Physics, University of the Basque Country, Lejona, Spain*

12 September 2018

## ABSTRACT

We show that the kinematics of the shells seen around some elliptical galaxies provide a new, independent means for measuring the gravitational potentials of elliptical galaxies out to large radii. A numerical simulation of a set of shells formed in the merger between an elliptical and a smaller galaxy reveals that the shells have a characteristic observable kinematic structure, with the maximum line-of-sight velocity increasing linearly as one moves inward from a shell edge. A simple analytic calculation shows that this structure provides a direct measure of the gradient of the gravitational potential at the shell radius. In order to extract this information from attainable data, we have also derived the complete distribution of line-of-sight velocities for material within a shell; comparing the observed spectra of a shell to a stellar template convolved with this distribution will enable us to measure the gradient of the potential at this radius. Repeating the analysis for a whole series of nested shells in a galaxy allows the complete form of the gravitational potential as a function of radius to be mapped out. The requisite observations lie within reach of the up-coming generation of large telescopes.

## 1 INTRODUCTION

The gravitational potentials of elliptical galaxies have proved difficult to derive, especially at large radii. In disk galaxies, both stars and gas have relatively simple orbit structures dominated by nearly circular orbits, and it is therefore straightforward to deduce the underlying gravitational potential (at least in the disk plane) from the observed kinematics in these systems. However, the corresponding orbital structure in elliptical galaxies is much more complicated, making the derivation of the gravitational potential from observed kinematics in such a system far from simple. In fact, basic kinematic observations of projected density and line-of-sight velocity dispersion are not sufficient to solve unambiguously for both the functional form of the gravitational potential and the distribution of stellar orbits in elliptical galaxies (Binney & Mamon 1982). This ambiguity has recently been partially resolved by using the extra kinematic information that can be derived from the shapes of line profiles in high quality spectral data (e.g. Gerhard 1993, Carollo et al. 1995). However, these results are restricted to the inner few effective radii of the stellar light; it is hard to extend these methods to much larger radii because of the low surface brightnesses of galaxies further out. Independent mass measurements using gravitational lensing (e.g. Kochanek 1995) are restricted to still smaller radii. The only technique that reaches to large radii comes from mapping the distribution of hot gas around some ellipticals (Buote & Canizares 1997). This method relies on the assumption of hydrostatic equilibrium in the analysis of X-ray

intensity and temperature profiles, from which the gravitational potential may be deduced. The requisite data are hard to obtain with current X-ray telescopes, and the analysis is subject to possible systematic uncertainties if the hot gas is not in a single phase. Furthermore, many of the X-ray halos may be associated with the group hosting the elliptical rather than with the galaxy itself. It is therefore of interest to develop alternative probes of the mass distribution in the outer parts of elliptical galaxies.

If we wish to measure the gravitational potential of an elliptical galaxy unambiguously using kinematic tracer particles, then we need a set of test bodies whose orbital structure is simple and observationally well-constrained. In this paper, we show that the large, regular systems of faint shells seen in some elliptical galaxies (Schweizer 1980, Malin & Carter 1980) offer just such a tracer. These shells are believed to be the remnants of a small galaxy after a head-on collision with a larger system – any other collision geometry does not result in extensive, nested shell systems. From the geometry of the merger, we know that all the stars in each shell must be on radial orbits with very similar energies. As we show below, this particularly-simple orbital structure means that the kinematics of the shells provide a useful new probe of the gravitational potential out to large radii in elliptical galaxies.

## 2 SHELL GALAXIES

Deep photometric observations reveal that around 10% of elliptical galaxies contain large numbers of faint concentric annular shells of enhanced starlight (Malin & Carter 1983, Schweizer 1983). A number of models have been proposed to explain the origin of these “shell galaxies.” For example, Fabian, Nulsen & Stewart (1980) have suggested that shock waves in the intergalactic medium could induce star formation with the observed shell-like structure, and Thomson (1991) modelled the shells as a type of spiral density wave excited by the passage of a companion galaxy. However, perhaps the most widely accepted model involves the merging of a small satellite with a large galaxy. In this paper we examine the implications of this model for the kinematics of shells.

### 2.1 The basic merger model

Numerical simulations have shown that when a small galaxy collides head-on with a larger system, a whole series of shell-like structures is formed (e.g. Quinn 1984). The small galaxy is disrupted by the tidal forces of the encounter, but the orbits that the liberated stars follow in their new host galaxy closely reflect the original motion of their progenitor galaxy. These stars hence find themselves on nearly radial orbits with similar initial positions and velocities. All of the stars were injected into the host galaxy at the same moment, but stars with slightly different energies follow orbits with slightly different periods, and so as time proceeds the merging stars slowly spread out along a path through the centre of the host galaxy.

As the stars approach the end of each radial excursion through the galaxy, they slow to a halt before reversing their path, leading to a large enhancement in stellar density at these points. Hence, only stars that lie close to the extreme ends of their orbits will contribute significantly to the surface brightness of the galaxy. At any given moment, only stars with particular orbital periods will have completed an integer number of radial excursions and thus find themselves at this phase of their orbits. The orbital periods correspond to particular energies, and so we only see stars with these quantized orbital energies. Since stars with different energies have orbits that take them to different extreme radii, we witness this phenomenon as a series of shells.

In summary, each shell is made up of stars from the destroyed galaxy with equal orbital energies. The shells at different radii contain stars with different energies, which therefore have completed different integer numbers of radial excursions since the merger. Since the stars in any shell have a very small velocity dispersion compared to that of their host galaxy, these structures show up very clearly as sharp edges in the photometry of the system.

### 2.2 Numerical simulations of shell kinematics

In order to examine the observable kinematic properties of the shells produced in a merger, we have carried out simulations in which an unbound satellite is accreted by a massive spherical galaxy. We adopted the isochrone potential,

$$\Psi(r) = -\frac{1}{1 + (1 + r^2)^{1/2}}, \quad (1)$$

for the host galaxy; since the action/angle variables of the orbits in such a potential can be calculated analytically (McGill & Binney 1990; Gerhard & Saha 1991), the time evolution of the orbits can be obtained in a single step without requiring full orbit integrations, and so it is computationally cheap to obtain snap-shot views of the evolution of such a system containing a large number of test particles. We modelled the initial configuration for the satellite with a Gaussian density profile (dispersion 0.5) and zero velocity dispersion. Figure 1 shows the shells produced 750 time units after such a satellite is released with zero velocity at radius  $r = 3$ .

Kinematically, what we might hope to observe are the line-of-sight velocities of the particles in each shell. Figure 2 shows the line-of-sight velocities of the particles as a function of position along the axis defined by the direction of the collision. Evidently, each shell has a characteristic projected velocity structure, with a sharp-edged double-peaked distribution whose width goes to zero at the shell edge. Below, we show why such profiles arise, and how they can be used as diagnostics of the underlying gravitational potential.

### 2.3 The kinematics of individual shells

The sharp velocity structures in a shell arises because the shell is made up of stars with only a small range of orbital energies. We might therefore hope to understand Figure 2 by treating each shell as a mono-energetic ensemble of stars on radial orbits. Figure 3 shows schematically the observable kinematics – density of stars as a function of line-of-sight velocity and position – for a cross-sectional view through one such shell. Clearly, the line-of-sight velocity of a star depends on its location with respect to the shell edge. Near the outer edge of the shell (point A in Fig. 3), stars are close to turning around in their orbits, and so their velocities will lie near the systemic velocity of the host galaxy. Similarly, stars near the tangent point (point B) move mostly transverse to the line of sight, also resulting in near-systemic observed velocities. At intermediate positions, stars do have finite line-of-sight velocities, however; moreover, on lines of sight further in from the shell edge, orbital speeds are larger resulting in larger line-of-sight velocities. The resulting distributions of velocity are sketched schematically in the lower panels of Fig. 3.

To derive the variation in maximum velocity with distance from the shell edge, consider a mono-energetic population of stars orbiting radially in the gravitational potential  $\Psi(r)$ . The stars form a shell whose outer edge lies at radius  $r = r_s$ . By energy conservation, the radial velocity of stars in this shell at radius  $r < r_s$  is simply

$$v_r = \pm (2[\Psi(r_s) - \Psi(r)])^{1/2}. \quad (2)$$

If  $R$  and  $z$  denote the projected radius of a line of sight probing the shell and the distance along this line respectively (with the host galaxy at  $z = 0$ ), then the line-of-sight velocity of this material,  $v_{\text{los}}$ , is given by

$$v_{\text{los}}^2 = \left(\frac{z}{r}v_r\right)^2 = 2 \left(1 - \frac{R^2}{r^2}\right) [\Psi(r_s) - \Psi(r)] \quad (3)$$

The maximum value for  $v_{\text{los}}^2$  along any given line of sight can be calculated approximately by expanding equation (3)

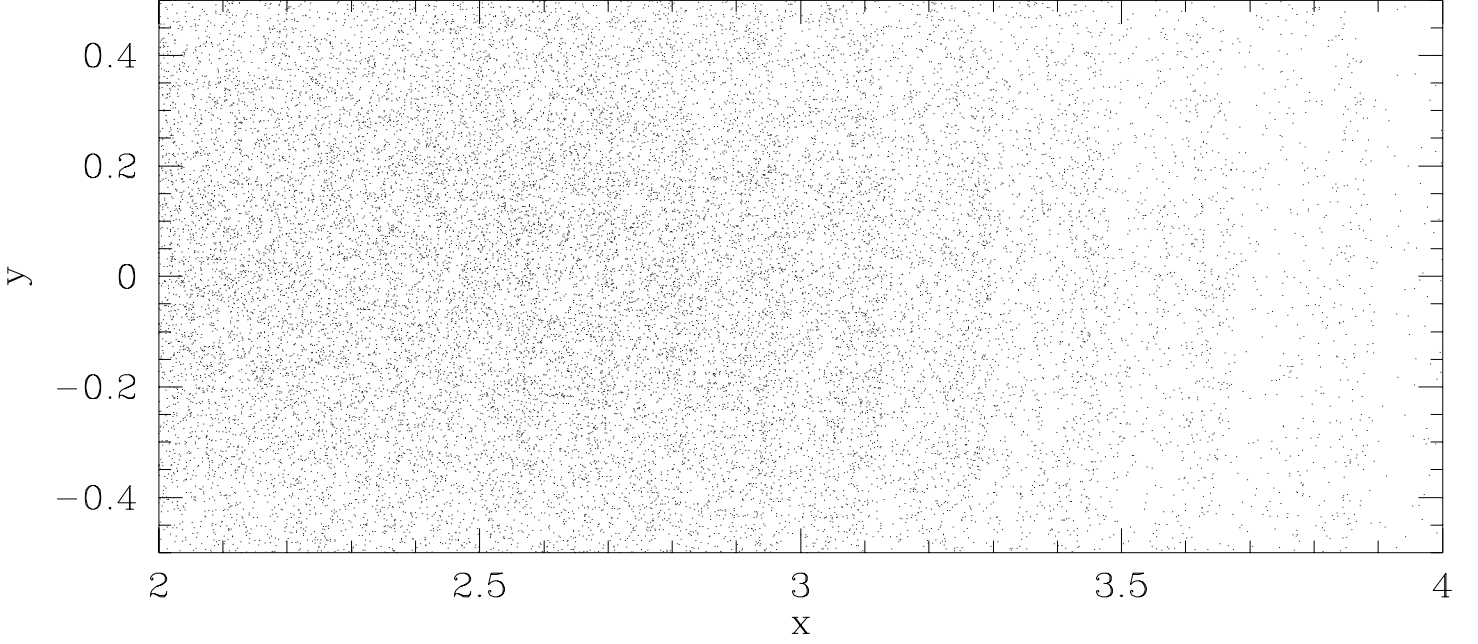


**Figure 1.** Projected density of part of the shell system generated by a small unbound satellite falling into a spherical isochrone potential.

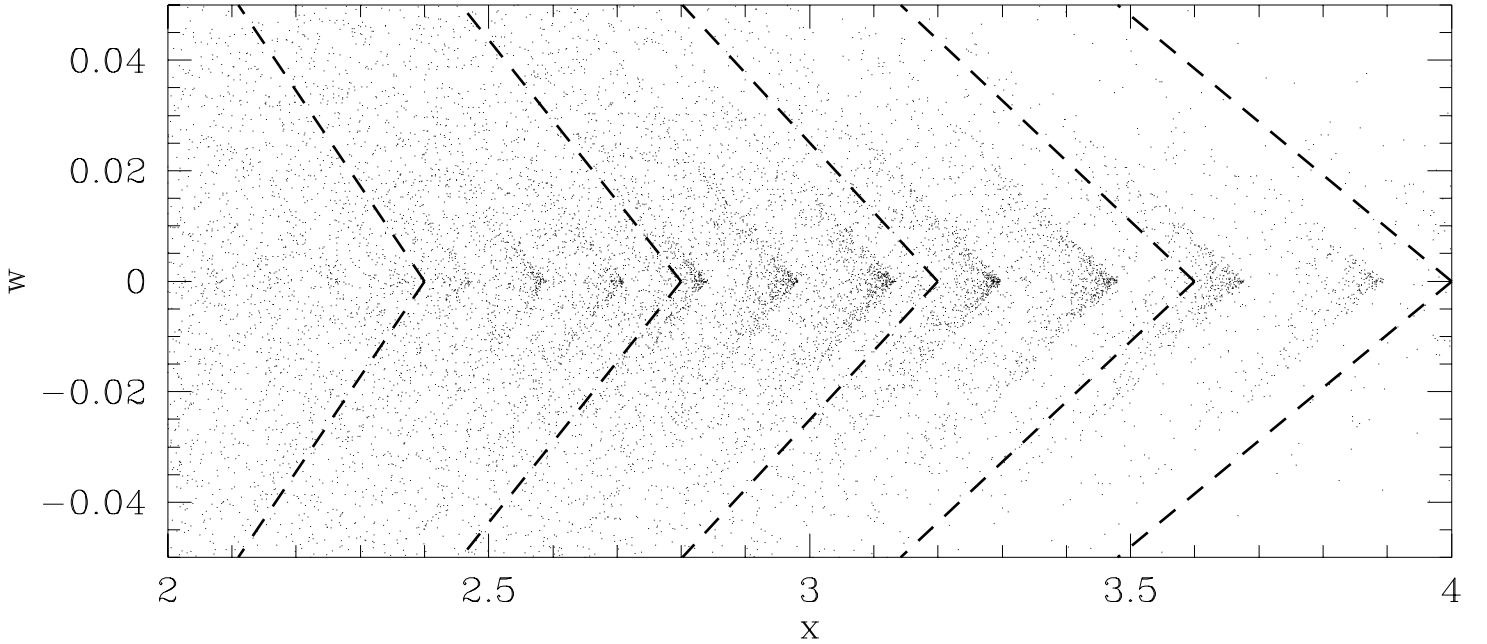


**Figure 2.** The velocity structure of the shells shown in Fig. 1. The slopes of the V-shaped line profiles agree well with the predictions of the approximate formula of equation (7) (shown as dashed lines).

about  $r = r_s$ :

$$\begin{aligned}
 v_{\text{los}}^2 &= -2(r - r_s)\Psi'(r_s) \left(1 - \frac{R^2}{r_s^2}\right) \\
 &\quad - (r - r_s)^2 \left( \frac{4R^2\Psi'(r_s) + r_s(r_s^2 - R^2)\Psi''(r_s)}{r_s^3} \right) \\
 &\quad + O[(r - r_s)^3].
 \end{aligned} \tag{4}$$

Along lines of sight close to the shell edge ( $|R - r_s| \ll r_s$ ), this expression reduces to

$$\begin{aligned}
 v_{\text{los}}^2 &= 4(r - r_s)[\Omega(r_s)]^2(R - r_s) - 4(r - r_s)^2\Omega(r_s)^2 \\
 &= 4(r_s - r)(r - R)[\Omega(r_s)]^2,
 \end{aligned} \tag{5}$$

where  $\Omega(r) = [\Psi'(r)/r]^{1/2}$  is the circular frequency at a radius  $r$ .

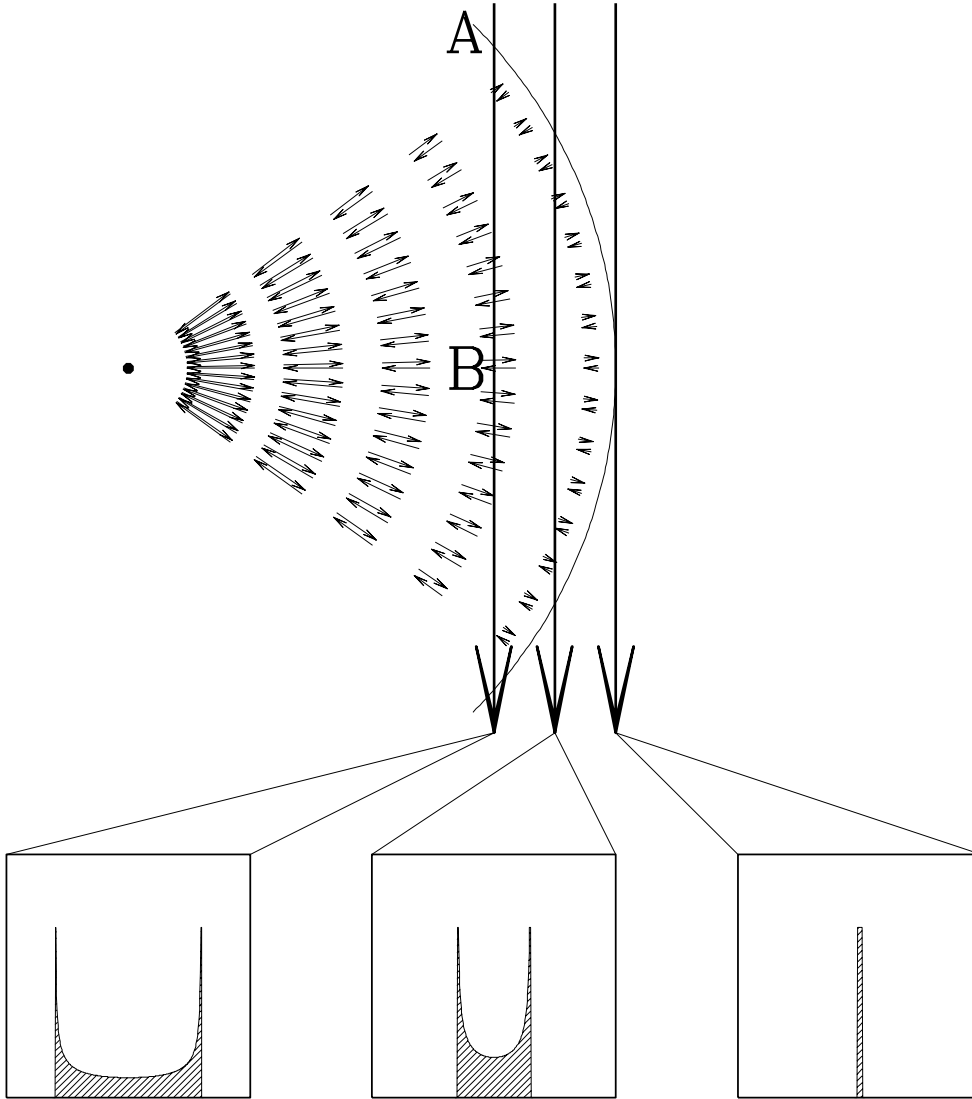


**Figure 3.** Schematic diagram showing the velocities of stars in a spherical shell system. The top part of the diagram shows a mono-energetic system of stars moving on radial orbits, and the inset figures show the distributions of these stars' line-of-sight velocities down three lines of sight.

For a given shell radius and line of sight,  $|v_{\text{los}}|$  is maximized at  $r = \frac{1}{2}(R + r_s)$ , where it has the value

$$v_{\text{max}} = \pm\Omega(r_s)(r_s - R). \quad (6)$$

In other words, the projected velocity width of a shell at projected radius  $R$ ,  $\Delta v_{\text{los}}(R) = 2|v_{\text{max}}|$  increases approximately linearly inwards from zero at the edge of the shell, with slope

$$\frac{d\Delta v_{\text{los}}}{dR} = -2\Omega(r_s). \quad (7)$$

Lines of this slope are plotted in Figure 2, and, indeed, match the extreme velocities of the shell features very well.

Since this slope is just the circular frequency at the radius of the shell, it provides direct information on the host galaxy's gravitational potential at this point. Measuring the slope for each of the shells then yields a series of measurements of the gradient of the galaxy's potential at different radii. These constraints can either be treated as direct measurements of the enclosed mass at different radii, or they

can be approximately numerically integrated over radius to obtain a direct measure of the gravitational potential.

In practice, it will be difficult to measure accurately the edges of the velocity distribution of a shell. What is actually seen in the spectrum of a shell is the convolution of a stellar spectrum with the line-of-sight velocity distribution (LOSVD) of the stars in the shell,  $F(v_{\text{los}})$ . In order to interpret spectra of shells, we need to know the shape of this function. The LOSVD can be calculated analytically for mono-energetic shells of stars on radial orbits as follows. The contribution to the distribution by a portion of shell material at distance  $z$  down the line of sight in an area of size  $A$  centered on projected radius  $R$  is given by:

$$F(v_{\text{los}})dv_{\text{los}} = \nu(r)Adz, \quad (8)$$

where:

$$z^2 = r^2 - R^2; \quad (9)$$

$$\nu(r) = \frac{k}{v_r r^2}; \quad (10)$$

$$v_r = [2(\Psi(r_s) - \Psi(r))]^{1/2}; \quad \text{and} \quad (11)$$

$$v_{\text{los}} = 2\Omega(r_s)[(r - R)(r_s - r)]^{1/2}. \quad (12)$$

A given value of  $|v_{\text{los}}|$  corresponds to two distinct radii,

$$r_{\pm} = \frac{1}{2} \left\{ R + r_s \pm [(r_s - R)^2 - \Omega(r_s)^{-2}v_{\text{los}}^2]^{1/2} \right\}, \quad (13)$$

so two contributions need to be added in order to calculate the line profile:

$$F(v_{\text{los}}) = \frac{kA|v_{\text{los}}|}{2\Omega(r_s)^2} \left( \frac{1}{r_+ z_+ v_{r_+} |R + r_s - 2r_+|} + \frac{1}{r_- z_- v_{r_-} |R + r_s - 2r_-|} \right), \quad (14)$$

where  $z_{\pm} = (r_{\pm}^2 - R^2)^{1/2}$ . Simplifying by expanding this equation about radius  $r = r_s$ , and assuming  $(r_s - R) \ll r_s$ , we obtain the LOSVD

$$F(v_{\text{los}}) \propto \frac{1}{[(r_s - R)^2 - \Omega(r_s)^{-2}v_{\text{los}}^2]^{1/2}}. \quad (15)$$

This two-horned profile, reminiscent of integrated HI profiles of disk galaxies, forms a single-parameter family of distributions. Some sample LOSVDs of this form are illustrated in Fig. 3. By convolving a stellar ‘‘template’’ spectrum with an LOSVD of this form, it will be possible to find the values for  $\Omega(r_s)$  that best reproduce the observed galaxy spectrum. By repeating this process for spectra of shells spanning a wide range in radii, it is thus possible to reconstruct the complete gravitational potential of the galaxy.

### 3 DISCUSSION

In this paper, we have set out to show how the kinematics of the shells produced when a small galaxy merges with a large system can be used to measure the underlying gravitational potential. As mentioned earlier in the paper, although the minor merger model is the most widely accepted interpretation of extensive shell systems, several other possible explanations have been advanced. Thus, not only would the detection of the characteristic kinematic structure illustrated

in Fig. 2 allow us to measure the gravitational potential, but it would also confirm the origin of the shells themselves.

An alternative method for using shells to constrain the form of the gravitational potential was originally proposed by Quinn (1984). He suggested that use be made of the distribution of shells with radius. Recall that, at any given time, the photometrically-observed shells are delineated by those stars that have completed integer number of radial oscillations. The ratio of the radii of successive shells therefore gives the oscillation periods at different energies, which is directly related to the form of the potential. The constraints on the potential obtained from such analyses are non-dimensional; they could, for example, provide information about the power-law index of the potential, but they cannot yield a mass normalization. By contrast, the kinematic method described here relies on measured velocities, which can be translated directly into the fully-dimensional gravitational potential. The shell counts have also been shown to be susceptible to uncertainties associated with dynamical friction acting on the shredding satellite, since different shells will have followed substantially different orbits, with different numbers of passages through the center of the host galaxy. Quinn’s method also requires that we know how many radial oscillations the outermost shell has executed, which can only be inferred indirectly. The method discussed here, on the other hand, only uses information from each shell singly, and only uses the fact that phase wrapping is an efficient mechanism for concentrating stars of very nearly equal energies.

Our analysis has assumed that the merger occurred on an exactly radial orbit. To test the importance of this assumption, we have repeated our simulations in the isochrone potential for satellite galaxies on slightly non-radial orbits. These calculations revealed that even in systems where the encounter is sufficiently off-axis to produce shells that do not appear regular and aligned, the line profiles of individual shells are still accurately reproduced by the radial model calculations. Thus, the kinematics of an aligned shell system will almost certainly be well-modelled by the simple radial orbit approximation. Furthermore, altering the viewing angle of the shell system tends to diminish the shell visibility before altering the velocity structure, again suggesting that by selecting aligned, regular shell systems, we will preferentially find systems to which the above analysis is applicable. It should be noted, however, that the tests we have carried out have all been based on the isochrone potential, since the orbit calculations are computationally simple in a potential of this form. It would be interesting to carry out a more extensive numerical study of shells in other potentials in order to check that they, too, are insensitive to the assumption of radial orbits.

Any flattening of the host galaxy’s potential is also a possible problem. It may introduce orientation-dependent effects, as well as modify the orbit structure of the stars making up each shell. Simulations of the type described earlier in flattened potentials show that regular shell systems only occur for nearly radial encounters in spherical potentials: a degree of flattening as small as 5% in the potential will cause significant beating between the motions in the various directions, and leads to shells with alternately large and small opening angles. The velocity structure of such shells is also rather disturbed, and it is not clear that the veloc-

ity profiles will provide much information about the overall potential. However, the detection of a regular uniform shell system provides us with strong *a priori* evidence that the potential must be very close to spherically-symmetric.

Shells are photometrically faint structures, and so obtaining the kinematic measurements that we advocate here will not be simple. It is, however, noteworthy from a comparison of Figs. 1 and 2 that the kinematic observation of these systems significantly enhances their contrast against any background. It is also worth noting that the brightnesses of observed shells do not decrease very rapidly with radius, and so, unlike other techniques for measuring gravitational potentials using stellar kinematics, the difficulty of applying this method does not increase prohibitively with radius. We have carried out signal-to-noise ratio calculations for some of the brighter shell galaxies such as NGC 3923, and have ascertained that data of the requisite quality could be obtained with a couple of nights' integration using a 4-metre telescope. Clearly, projects of this nature will prove quite feasible with the up-coming generation of large telescopes.

#### ACKNOWLEDGEMENTS

This paper was completed during a visit to the Lorentz Centre at the University of Leiden, and the authors gratefully acknowledge the hospitality of this institution. MRM is supported by a PPARC Advanced Fellowship (B/94/AF/1840).

#### REFERENCES

- Binney, J. & Mamon, G.A., 1982, MNRAS, 200, 361  
 Buote, D.A. & Canizares, C.R., 1997, ApJ, 474, 650  
 Carollo, C.M., de Zeeuw, P.T., van der Marel, R.P., Danzinger, I.J. & Qian, E.E., 1995, ApJ, 441, L25  
 Fabian, A.C., Nulsen, P.E.J. & Stewart, G.C., 1980, Nat, 287, 613  
 Gerhard, O.E. 1993, MNRAS, 265, 213  
 Gerhard, O.E. & Saha, P., 1991, MNRAS, 251, 449  
 Kochanek, C.S., 1995, ApJ, 445, 559  
 Malin, D.F. & Carter, D., 1980, Nat, 285, 643  
 Malin, D.F. & Carter, D., 1983, ApJ, 274, 534  
 McGill, C. & Binney, J., 1990, MNRAS, 244, 634  
 Quinn, P.J., 1984, ApJ, 279, 596  
 Schweizer, F., 1983, in IAU Symposium 100, Internal Kinematics and Dynamics of Galaxies, ed. E. Athanassoula (Dordrecht: Reidel)  
 Schweizer, F., 1980, ApJ, 237, 303  
 Thomson, R.C., 1991, MNRAS, 253, 256